


ORIGINAL RESEARCH ARTICLE

In vitro biomechanical properties of porcine perineal tissues to better understand human perineal tears during delivery

Marine Lallemand^{1,2}  | Tiguida Kadiakhe² | Jérôme Chambert² | Arnaud Lejeune² | Rajeev Ramanah^{1,3} | Nicolas Mottet^{1,3} | Emmanuelle Jacquet²

¹Department of Gynecology and Obstetrics, Besançon University Medical Center, Besançon, France

²Department of Applied Mechanics, FEMTO-ST Institute, University of Franche-Comte, UMR 6174 CNRS, Besançon, France

³Nanomedicine Imaging and Therapeutics Laboratory, INSERM EA 4662, University of Franche-Comte, Besançon, France

Correspondence

Marine Lallemand, Service de Gynécologie-Obstétrique, CHU Besançon, bd Alexandre Fleming, 25000 Besançon, France.

Email: marine.lallemand@wanadoo.fr

Abstract

Introduction: Data concerning the mechanical properties of the perineum during delivery are very limited. In vivo experiments raise ethical issues. The aim of the study was to describe some of the biomechanical properties of each perineal tissue layer collected from sows in order to better understand perineal tears during childbirth.

Material and methods: Samples of each perineal tissue layer were obtained from the skin, the vagina, the external anal sphincter (EAS), the internal anal sphincter (IAS), and the anal mucosa of fresh dead sows. They were tested in quasi-static uniaxial tension using the testing machine Mach-1®. Tests were performed at a displacement velocity of 0.1 mm·s⁻¹. Stress–strain curves of each perineal tissue layer before the first damage for each sow were obtained and modeled using a hyperelastic Yeoh model described by three coefficients: C1, C2, and C3. Pearson correlation coefficients were calculated to measure the correlation between the C1 hyperelastic coefficient and the duration between the first microfailure and the complete rupture for each perineal tissue layer. Pearson correlation was computed between C1 and the number of microfailures before complete rupture for each tissue.

Results: Ten samples of each perineal tissue layer were analyzed. Mean values of C1 and corresponding standard deviations were 46 ± 15, 165 ± 60, 27 ± 10, 19 ± 13, 145 ± 28 kPa for the perineal skin, the vagina, the EAS, the IAS, and the anal mucosa, respectively. According to this same sample order, the first microfailure in the population of 10 sows appeared at an average of 54%, 27%, 70%, 131%, and 22% of strain. A correlation was found between C1 hyperelastic coefficient and the duration between the first microfailure and the complete rupture ($r=0.7$, $p=0.02$) or the number of microfailures before complete rupture only for the vagina ($r=0.7$, $p=0.02$).

Conclusions: In this population of fresh dead sow's perineum, the vagina and the anal mucosa were the stiffest tissues. The IAS and EAS were more extensible and less stiff. A significantly positive correlation was found between C1 and the duration between

Abbreviations: EAS, external anal sphincter; IAS, internal anal sphincter.

This is an open access article under the terms of the [Creative Commons Attribution-NonCommercial-NoDerivs](https://creativecommons.org/licenses/by-nc-nd/4.0/) License, which permits use and distribution in any medium, provided the original work is properly cited, the use is non-commercial and no modifications or adaptations are made.

© 2024 The Authors. *Acta Obstetrica et Gynecologica Scandinavica* published by John Wiley & Sons Ltd on behalf of Nordic Federation of Societies of Obstetrics and Gynecology (NFOG).

the first microfailure and the complete rupture of the vagina, and the duration between the first microfailure and the complete rupture of the vagina.

KEYWORDS

biomechanical properties, childbirth, deformation, perineal tear, perineum, rupture, stress-strain curve

1 | INTRODUCTION

The perineum is a soft structure made up of skin and muscles closing the pelvis. It is located under the levator ani muscle. Its mechanical properties ensure normal pelvic stability. During childbirth, the morphological and dynamic adaptation of the perineum to fetal presentation depends on its resistance to the stresses induced by the presentation. Under the compressive efforts induced by fetal presentation, the perineum becomes thinner until, sometimes, it tears. This can lead to more or less severe perineal tears. Third- and fourth-degree tears correspond to obstetrical lesions of the anal sphincter and/or anal mucosa. These perineal lacerations can impact women's quality of life with anal incontinence, perineal pain, dyspareunia, recto-vaginal fistula, and depression.^{1,2} The rate of obstetrical anal sphincter injuries varies between 0.25% and 6% depending on the study.³

Data concerning the mechanical properties of the perineum and fetal stresses during delivery are very limited.⁴⁻¹⁰ They result essentially from numerical models of the distension of the levator ani muscles. Only Zemčik et al. managed to quantify perineal strain during vaginal delivery using stereophotogrammetry.¹⁰ However, the perineum is a structure composed of different tissues whose behavior must be characterized in order to understand the tearing mechanism. Knowledge of the biomechanical parameters of the perineum is necessary to understand perineal tears, but *in vivo* experimentation raises ethical issues. To begin our work, we studied the biomechanical properties of porcine perineum. A porcine model was chosen because of its similar morphological and immunohistochemical properties, and the results of microindentation tests as reported in the literature.^{11,12} The aim of our study was to describe some of the biomechanical properties of each perineal tissue layer collected from sows in order to better understand perineal tears during childbirth.

2 | MATERIAL AND METHODS

We performed an experimental study on porcine perineal tissues. Ten samples of each perineal layer were analyzed. They were dissected from fresh dead sows provided by local slaughterhouse waste. The sow breed was the French butcher pig. Sows were slaughtered 24–48h before the experimentation; they were not frozen. For each sow, one sample was obtained from the skin perineal layer, the vagina perineal layer, the external anal sphincter (EAS), the internal anal sphincter (IAS), and the anal mucosa perineal layer (Figures 1 and 2).

Key message

C1 hyperelastic coefficients of perineal tissues (fresh dead sow) were ranked in ascending order: IAS, EAS, skin, anal mucosa, and vagina. Similar human results could explain anal sphincter integrity and isolated rectal buttonhole perineal tears in childbirth.

Sows were refrigerated before sample collection. In order to obtain samples in a reproducible way and preserve fiber integrity, a precise dissection method was implemented (Figure 2). The dissection was performed by a urogynecologist who was expert in the anatomy of perineal tears. Instruments used were fine scissors and atraumatic forceps. No traction was exerted on the tissues. A careful midline incision next to the vulvar area between the vaginal and anal openings was made. The EAS was immediately identified and isolated. The perineal skin was dissected from the anus to the ventral extremity into two dorso-ventral samples (right and left). Next, the ventral part of the vagina was incised at 6 o'clock to facilitate vaginal access. Right and left vaginal samples from the perineum were dissected on the rectovaginal septum side. Histologically, the vaginal sample included the vaginal wall composed of mucosa, lamina propria, muscularis, and adventitia. Then, the EAS was carefully dissected and sectioned at 9 o'clock and 3 o'clock. Finally, the dorsal wall of the rectum and anus was incised at 12 o'clock. Two samples (right then left) of the anal mucosa and the IAS were obtained. Only the samples on the right side were analyzed for the perineal skin, the perineal vagina, the perineal anal mucosa, and the IAS. The left samples of these sows were analyzed in another study with non-comparable experimental conditions. EAS was taken. The entire EAS was collected between the vagina and the anus. Due to its thinness, it was not possible to divide it into two samples like the other layers. The entire EAS was used for sampling, along the fibers, in this study. Samples were oriented (dorso-ventral, left-right, cranio-caudal).

To obtain uniform stresses at the center of the sample during tensile testing, standardized samples were cut for each perineal layer with a scalpel and a caliper. Samples were obtained using a rectangular pattern 30mm long and 10mm wide in the cranio-caudal direction for all tissues except the EAS, which was in the latero-lateral direction (direction shown in Figure 3).

Each sample end was covered with instant glue (Loctite 401®) and held in paper. These ends were inserted into the jaw of the

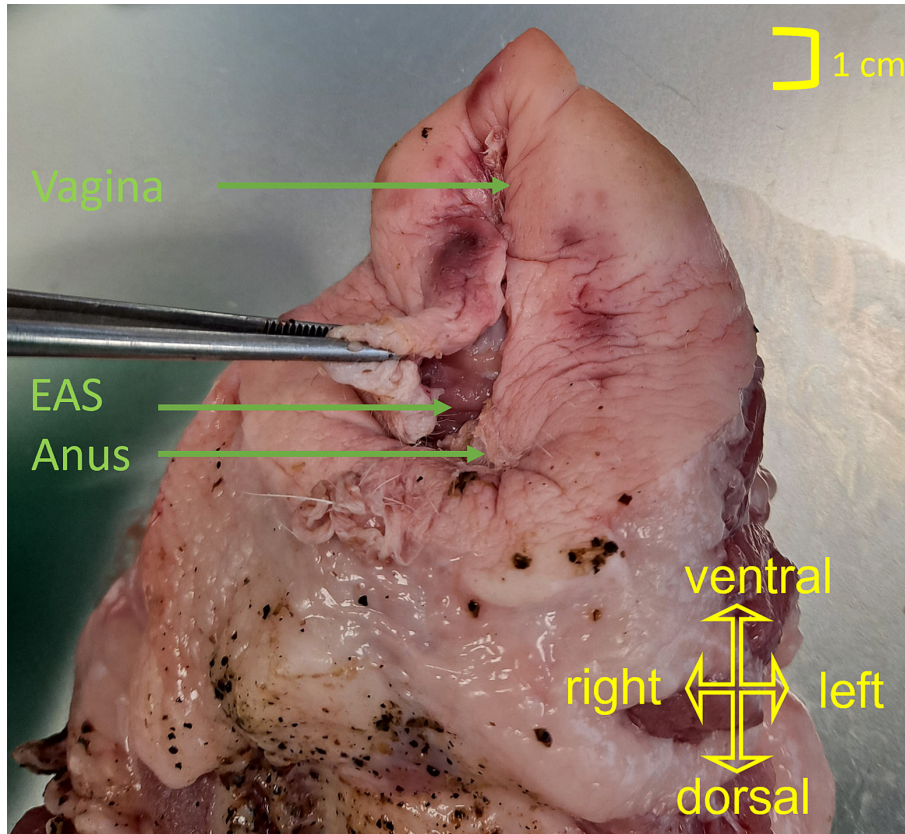


FIGURE 1 Anatomy of the sow's perineum. An incision of the perineal skin between the vagina and the anus was performed to reveal the external anal sphincter (EAS).

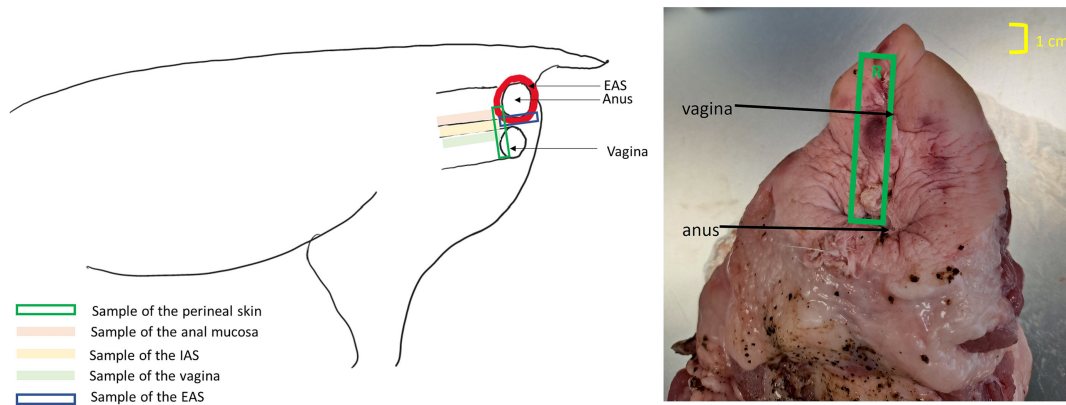


FIGURE 2 Obtention of the skin, the vagina, the IAS, the EAS and the anal mucosa samples of the sow. EAS, external anal sphincter; IAS, internal anal sphincter.

mechanical tester in such a way as not to over- or under-tighten (Figure 3). If the sample slipped, it would not be taken into account in the post-processing analysis.

Uniaxial tensile tests were carried out using a Mach-1® mechanical tester (Biomomentum Inc., Canada). Tensile forces, stretching forces acting on the tissue, were measured with a 250-N cell. A preload of 0.3N was applied for 2 min before each test to compare sample results. Sample sizes were measured after the pre-stress. Initial measurements of thickness (t_0), width (w_0), and length (l_0) were obtained using a digital caliper after preload in the middle of the sample

to avoid compression tissue and deformation near the jaws. The moving crosshead displacement (Δl) of the tensile-testing machine was recorded to an accuracy of 0.5 μm in the direction of stress (traction), along with force at a frequency of 100Hz. Displacement was applied until failure. Tensile tests stopped when the sample broke. The tests were performed at a displacement velocity of 0.1 $\text{mm}\cdot\text{s}^{-1}$ and at a constant temperature of 21°C to avoid dehydration.

The uniaxial engineering stress σ (kPa) in the loading direction was defined by:

$$\sigma = \frac{F}{A_0} = \frac{F}{t_0 \cdot w_0}$$



FIGURE 3 Test machine Mach-1® (Biomomentum Inc, Canada) and grips for soft tissues.

where F is the measured force and A_0 is the initial cross-sectional area of the specimen.

The uniaxial engineering strain ε (%) in the loading direction is obtained by:

$$\varepsilon = \frac{\Delta l}{l_0}$$

Stress–strain curves of each perineal tissue before the first damage for each sow and their mean were obtained. Unlike elastic materials, where stress varies linearly with respect to strain, soft tissues are hyperelastic. This means that these tissues have a non-linear elastic behavior.¹³ Like elasticity, hyperelasticity models reversible behavior. Non-linearity allows large deformations to be taken into account. Non-linear elastic behavior of these tissues was observed and modeled using a Yeoh model¹⁴:

$$\Psi = \sum_{i=1}^3 C_i (I_1 - 3)^i$$

This hyperelastic law is described by three coefficients: C_1 , C_2 , and C_3 . These coefficients were identified by the method of least mean squares from experimental curves using the Levenberg–Marquardt algorithm before the initial sign of damage appeared in each tissue sample.¹⁵ The damage, also called microfailure, is the result of local and microscale effects. Occurrence of damage results in the weakening of the tissue and makes it more likely to rupture and tear. A microfailure is associated with the inflection point on the experimental curve and is identified by locating the maximum on the derivative of the curve. The inflection of the curve shows a reduction in the tissue's ability to withstand mechanical stress, which is interpreted by the appearance of fiber rupture or delaminations in the tissue. This inflection generally precedes macroscopic tissue rupture.

Only the C_1 hyperelastic coefficients were analyzed because of their meaning: initial slope of stress–strain curve at low strains (<5%). A high C_1 hyperelastic coefficient means that the tissue is

stiff (rigid) with a small deformation in response to an applied force. In contrast, a low C_1 hyperelastic coefficient means that the tissue is easy to deform even in response to a low applied force.

Tangent modulus (kPa) E_0 and E_1 were calculated for low and high strain, respectively. For each tissue, the mean stress and the mean strain were calculated up to the first rupture among all curves for the same tissue. Low strain was defined at the beginning of the master (mean) curve and used to define E_0 , i.e. at 0.4% deformation on average. E_1 was defined as the tangent modulus of the curve at the end of the mean curve, i.e. at 59% deformation on average. Minimum and maximum values of E_0 and E_1 were calculated from the lowest curve and the highest curve for each layer of perineal tissue, respectively.

Coefficients were expressed as mean \pm standard deviation. C_1 hyperelastic coefficients were compared according to the perineal layer using an analysis of variance model. If a statistically significant difference was found, pairwise comparisons using t tests and including Bonferroni correction were performed to identify which perineal layers were different from the others. In order to determine whether the C_1 hyperelastic coefficient was predictive of tissue damage, the Pearson correlation coefficient was calculated to measure the correlation between the C_1 hyperelastic coefficient and the duration between the first microfailure and the complete rupture for each tissue. Pearson correlation was computed between the C_1 hyperelastic coefficient and the number of microfailures before complete rupture for each tissue. Statistical analysis was performed using R software (version 4.3.0). For all analyses, we considered a p value less than 0.05 to be statistically significant.

3 | RESULTS

Ten samples of each layer were analyzed. Samples are described in Table 1. No sample slipped. Mean values of the C_1 hyperelastic coefficient and corresponding standard deviations were 46 ± 15 , 165 ± 60 , 27 ± 10 , 19 ± 13 , 145 ± 28 kPa for the perineal skin,

TABLE 1 Description of samples and tensile tests for each perineal tissues.

Tissue	Sample length (mm)	Sample width (mm)	Sample mean thickness (mm)	Temperature (°C)	Hygrometry (%)
Skin (n=10)	37±3	8±1	8±2	21±0.2	45±12
Vagina (n=10)	36±3	8±1	5±2	21±0.3	44±11
EAS (n=10)	34±4	8±4	7±2	21±0.3	44±12
IAS (n=10)	37±4	10±2	8±3	21±0.2	44±12
Anal mucosa (n=10)	36±3	7±1	4±1	21±0.2	44±11

Note: Results are expressed as mean ± standard deviation. The sample size measurements correspond to those obtained after the initial preload. Abbreviations: EAS, external anal sphincter; IAS, internal anal sphincter.

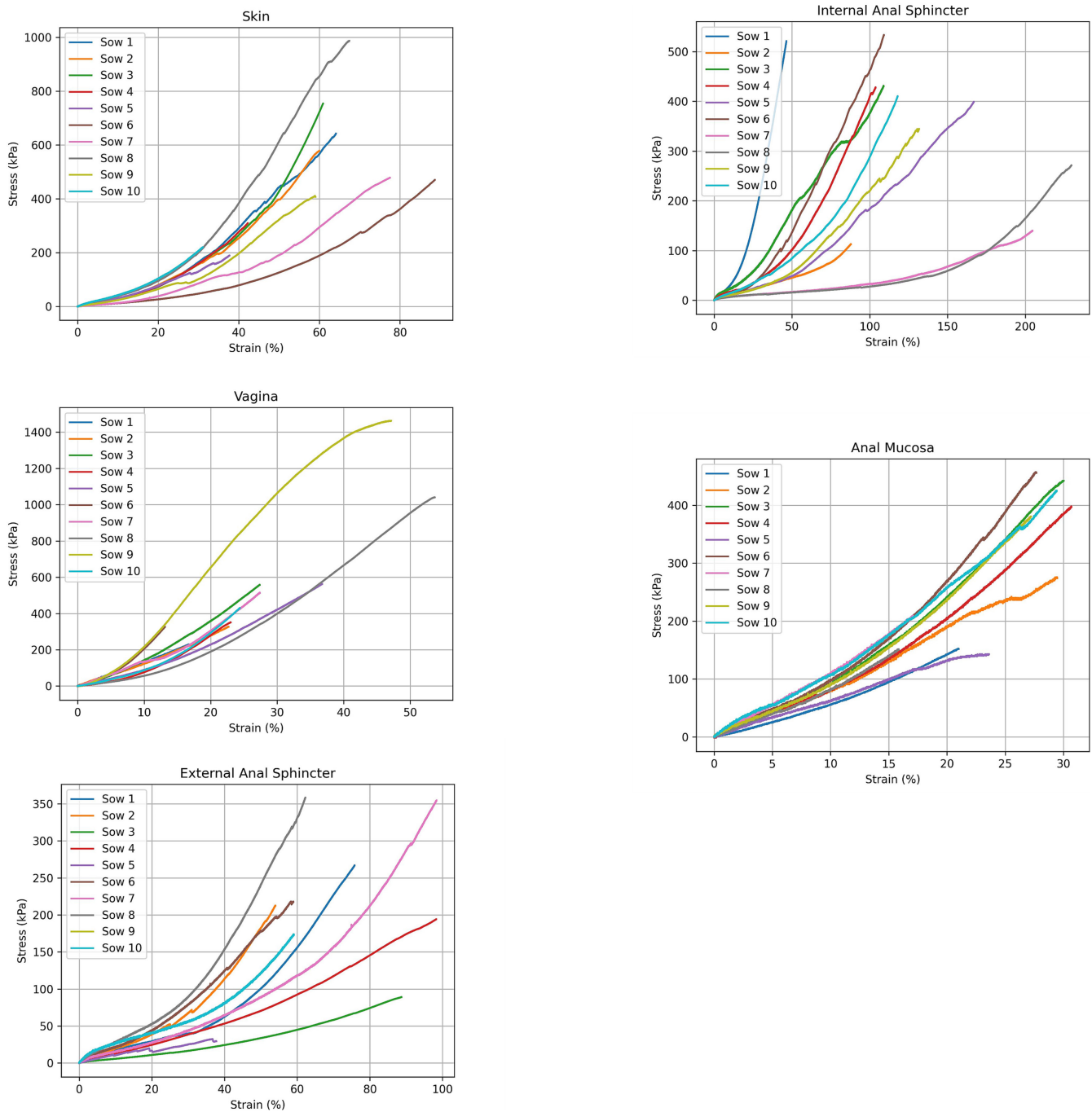


FIGURE 4 Stress–strain curves of each perineal tissue before first damage for each sow.

the vagina, the EAS, the IAS, and the anal mucosa, respectively (Figure 4; Table 2). C1 hyperelastic coefficients were statistically different between perineal layers ($p < 0.001$; Appendix S1). C1

TABLE 2 Hyperelastic coefficients according to the perineal tissue (Yeoh model).

Tissue	C1 (kPa)	C2 (kPa)	C3 (kPa)
Skin ($n = 10$)	46 ± 15	112 ± 69	13 ± 50
Vagina ($n = 10$)	165 ± 60	1285 ± 1424	-3137 ± 5702
EAS ($n = 10$)	27 ± 10	18 ± 29	8 ± 17
IAS ($n = 10$)	19 ± 13	47 ± 97	-13 ± 38
Anal mucosa ($n = 10$)	145 ± 28	215 ± 401	1152 ± 2818

Note: Results are expressed as mean ± standard deviation.

Abbreviations: EAS, external anal sphincter; IAS, internal anal sphincter.

TABLE 3 Parameter values from experimental stress–strain curves according to the perineal tissue (Yeoh model): E0 and E1 tangent modulus, Stress (kPa) at the first microfailure, Strain (%) at the first microfailure (minimum value, average value).

Tissue	E0 mean (min; max) (kPa)	E1 mean (min; max) (kPa)	Stress at first microfailure (kPa)	Strain at first microfailure at least	First microfailure at an average of
Skin ($n = 10$)	299 (247; 319)	907 (226; 1024)	603 ± 277	29%	54 ± 16% of strain
Vagina ($n = 10$)	830 (277; 711)	2250 (253; 651)	869 ± 339	13%	27 ± 13% of strain
EAS ($n = 10$)	332 (133; 502)	435 (40; 1026)	271 ± 163	38%	70 ± 21% of strain
IAS ($n = 10$)	253 (203; 621)	334 (279; 843)	428 ± 172	46%	131 ± 55% of strain
Anal mucosa ($n = 10$)	1108 (477; 1254)	1322 (573; 3067)	370 ± 144	14%	22 ± 6% of strain

Note: Results are expressed as mean ± standard deviation. For each tissue, the mean stress and the mean strain were calculated up to the first rupture among all curves for the same tissue. Low strain was defined at the beginning of the master (mean) curve and used to define E0. E1 was defined as the tangent modulus of the curve at the end of the mean curve. Minimum E0 and E1 were calculated from the lowest curve for each layer of perineal tissue. Maximum E0 and E1 were calculated from the highest curve for each layer of perineal tissue.

Abbreviations: EAS, external anal sphincter; IAS, internal anal sphincter.

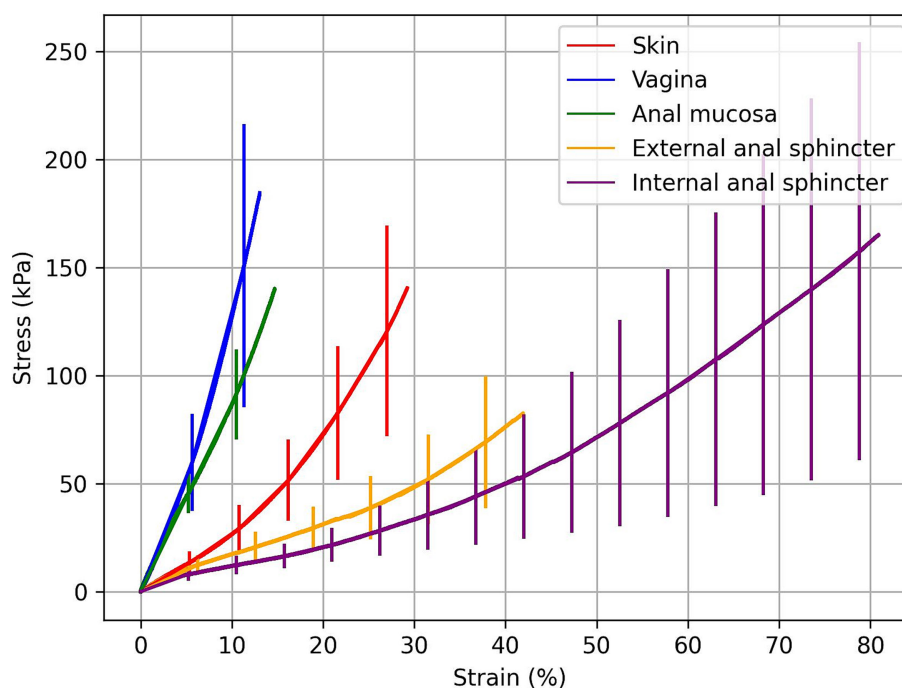


FIGURE 5 Mean stress–strain curves and their standard deviation for each perineal tissue before the first damage in this population ($n = 10$ for each perineal layers).

hyperelastic coefficients of the anal mucosa were statistically different from the C1 hyperelastic coefficients of the perineal skin, the EAS, and the IAS ($p < 0.001$). C1 hyperelastic coefficients of the perineal vagina were statistically different from the C1 hyperelastic coefficients of the perineal skin, the EAS, and the IAS ($p < 0.001$). The other perineal layers had statistically comparable C1 hyperelastic coefficients.

The vagina and the anal mucosa had the highest C1 hyperelastic coefficients. The mean ratio of C1 hyperelastic coefficients of the vagina to the anus was 0.3 (standard deviation of 0.1). The EAS and IAS had the lowest hyperelastic coefficients. Tensile tests lasted <15 min for the IAS and <10 min for the other perineal layers.

Tangent moduli during low and high strain are presented in Table 3. The E1 modulus derived from the mean of the curves tended to triple compared with the E0 modulus for the skin and the vagina.

Modulus E1 increased by a factor of 1.3 for EAS and IAS and by a factor of 1.2 for the anal mucosa.

The mean stress–strain curves and their standard deviations for each perineal tissue before the first damage in this population were drawn (Figure 5). The first microfailure in the population of 10 sows appeared at 29%, 13%, 38%, 46%, and 14% of strain for the perineal skin, the vagina, the EAS, the IAS, and the anal mucosa, respectively (Table 4). The first microfailure in the population of 10 sows appeared at an average of 54%, 27%, 70%, 131%, and 22% of strain for the perineal skin, the vagina, the EAS, the IAS, and the anal mucosa, respectively. The EAS and IAS were the most extensible and least stiff tissues. The vagina was the stiffest tissue. The anal mucosa was the least extensible tissue.

The durations between the first microfailure and the complete rupture of each tissue were 79 ± 105 , 69 ± 86 , 146 ± 168 , 151 ± 162 , 166 ± 108 s for the perineal skin, the vagina, the EAS, the IAS, and the anal mucosa, respectively (Table 5). The number of microfailures before complete rupture of each tissue was 16 ± 14 , 6 ± 4 , 23 ± 19 , 18 ± 17 , 38 ± 23 for the perineal skin, the vagina, the EAS, the IAS, and the anal mucosa, respectively (Table 5). The mean ratio of vaginal to anal microfailures before complete rupture was 0.2 (standard deviation 0.2).

A significantly positive correlation was found between the C1 hyperelastic coefficient and the duration between the first microfailure and the complete rupture of the vagina ($r=0.7$ $p=0.02$; Table 4). A significantly positive correlation was also found between the C1 hyperelastic coefficient and the duration between the first microfailure and the complete rupture of the vagina ($r=0.7$ $p=0.02$; Table 5).

For the others tissues, no correlation was found between the C1 hyperelastic coefficient and the duration between the first microfailure and the complete rupture of each tissue ($p>0.05$; Table 4). Also, there was no correlation between the C1 hyperelastic coefficient and the number of microfailures before complete rupture of each tissue except for vagina ($p>0.05$; Table 5).

4 | DISCUSSION

In this study, some biomechanical properties of each perineal layer of the sow have been obtained. C1 hyperelastic coefficients for perineal skin, the vagina, the EAS, the IAS, and the anal mucosa of fresh dead sow were measured.

In this population, the vagina and the anal mucosa were the stiffest. In other words, these rigid tissues had smaller deformation in response to an applied force. C1 hyperelastic coefficients of the vagina and the anal mucosa were higher than those of the perineal skin (165 and 145 kPa vs 46 kPa). This difference was also described by Gabriel et al., who compared the hyperelastic coefficient at low strain of the vagina and the abdominal skin of unfrozen cadavers without relevant pelvic organ prolapse (0.35 vs 0.14 MPa, $p>0.05$).¹⁶ In the literature, no study assessed the biomechanical properties of the anal mucosa. Only one rectal tissue evaluation was found.¹⁷ Rubod et al. compared vaginal and rectal tissue of fresh female cadavers without prolapse by performing multiaxial tension tests.¹⁷ They demonstrated that the vagina was much more rigid and less extensible than the rectal tissue. In our study, the anal mucosa and

Tissue	ΔT (s)	C1 (kPa)	Pearson's correlation
			r [95% CI]; p value
Skin ($n=10$)	79 ± 105	46 ± 15	0.4 [-0.3 to 0.8]; 0.2
Vagina ($n=10$)	69 ± 86	165 ± 60	0.7 [0.2 to 0.9]; 0.02
EAS ($n=10$)	146 ± 168	27 ± 10	0.2 [-0.6 to 0.7]; 0.7
IAS ($n=10$)	151 ± 162	19 ± 13	0.2 [-0.5 to 0.7]; 0.6
Anal mucosa ($n=10$)	166 ± 108	145 ± 28	0.2 [-0.4 to 0.7]; 0.5

Note: ΔT : duration between the first microfailure and the complete rupture. Results are expressed as mean \pm standard deviation unless otherwise stated.

Abbreviations: CI, confidence interval; EAS, external anal sphincter; IAS, internal anal sphincter.

TABLE 4 Correlation between C1 hyperelastic coefficient and the duration (ΔT) between the first microfailure and the complete rupture of each tissue (Yeoh model).

Tissue	Number of microfailures	C1 (kPa)	Pearson's correlation,	
			r [95% CI]	P value
Skin ($n=10$)	16 ± 14	46 ± 15	0.3 [-0.4 to 0.8]	0.5
Vagina ($n=10$)	6 ± 4	165 ± 60	0.7 [0.2 to 0.9]	0.02
EAS ($n=10$)	23 ± 19	27 ± 10	0.3 [-0.4 to 0.8]	0.4
IAS ($n=10$)	18 ± 17	19 ± 13	-0.3 [-0.8 to 0.4]	0.4
Anal mucosa ($n=10$)	38 ± 23	145 ± 28	0.2 [-0.5 to 0.7]	0.6

Note: Results are expressed as mean \pm standard deviation unless otherwise stated.

Abbreviations: CI, confidence interval; EAS, external anal sphincter; IAS, internal anal sphincter.

TABLE 5 Correlation between C1 hyperelastic coefficient and the number of microfailures before complete rupture of each tissue (Yeoh model).

the vagina were the least extensible tissues. Their first microfailure appeared at mean strains of 22% and 27%, respectively.

The IAS and EAS were the more extensible and the least stiff. The EAS is a skeletal muscle. Passive extensibility of skeletal muscles is an important component of total muscle function. It is well described in the literature.¹⁸ Studies with animal muscles have shown that passive extensibility is influenced by the size (mass) and length of muscle fibers, and the amount and arrangement of the connective tissues of the muscle belly. The resistance to passive lengthening is influenced by the readily adaptable amount of muscle tissue, including the contractile proteins and the non-contractile proteins of the sarcomere cytoskeletons.

Concerning the biomechanical properties of the IAS, no study was found in the literature. But a corroboration with vaginal smooth muscle cells could be made. Smooth muscle cells contribute to the quasistatic and viscoelastic mechanical behavior of soft tissues.¹⁹⁻²¹ According to Clark-Patterson et al., smooth muscle cells provide mobility by allowing the vagina to stretch under sustained pressures. In the same way, IAS could ensure mobility by allowing the anal mucosa to stretch under sustained pressures.²²

According to the tangent moduli, the skin and vagina seemed more resistant to deformation for high strain (much higher modulus). The stress applied to the tissues increased very quickly in the high strain zone, which tends to show that these tissues will tear first during childbirth because the deformations of the perineal tissues are imposed by the passage of the fetus. The great ability of EAS and IAS for deformation (38% and 46%) is highlighted by lower values of the E1 modulus for these tissues. The stresses applied were lower for the same level of deformation than those observed for the skin and the vagina. These data are compatible with what is observed in maternity wards. The skin and the vagina tend to tear first before the anal sphincter and the anal mucosa during childbirth.

In our study, the sow's anal sphincter was more extensible and less stiff than the vagina or the perineal skin. This could explain why severe perineal tears are rare in sows. If the same results are confirmed in humans, that could also explain why the anal sphincter is not always torn during childbirth. In the same way, the sow's anal mucosa and its vagina were the less extensible tissues. If these biomechanical properties are also found in humans, it could maybe explain the isolated rectal buttonhole perineal tear in obstetrics.²³ This is an isolated tear of the anal epithelium or rectal mucosa and vagina, but without involving the anal sphincter. This kind of laceration is rare in humans and only described in equine case reports.²⁴⁻²⁶

Concerning the experimental methodology, no failure or tears near the jaws were noticed. Operators trained before starting the study to avoid the learning phase and reduce these kinds of failure. Perineal stresses during delivery are not unidirectional. However, due to the size of the samples, only unidirectional traction tests at constant speed were performed. The Yeoh model was chosen because it accurately described the behavior of all the different perineal tissues. A comparison of the Yeoh, Mooney-Rivlin, and Ogden models on pig skin (belly and back) confirmed that the Yeoh model accurately

captures the behavior of the pig skin.²⁷ It also highlighted the stability issues that arise when using the Ogden model as well as the failure of the Mooney-Rivlin model to properly describe the behavior of the tissues. Moreover, it requires a small number of parameters, its first parameter being interpreted as half the initial shear modulus.

To our knowledge, our study is the first one in the literature to attempt to describe the biomechanical properties of each perineal layer in order to better understand perineal tears. This study focused on deformation. It concerns only the different tissues of the perineum, considered independently. This work is a preliminary step towards understanding the mechanisms involved. The next steps are aimed at identifying predictive parameters for the risk of perineal tears. These results could be used in simulations using the Finite Element Model. Structural tests on the whole perineum are currently underway, and will be used to validate the model of the whole perineum with controlled boundary conditions. This ongoing study aims to identify predictive parameters for the risk of failure associated with extreme loading conditions (>250% deformation).

According to Rosenberg and Trevathan, non-human primates have the most similar pelvic anatomy to humans.²⁸ However, their availability and cost have led us to seek another animal model. Ewes could have been used, but their availability remains difficult.^{29,30} Horses, which have a perineal body and are also subject to obstetrical anal sphincter injuries could also be an animal model.³¹ However, that model is difficult to obtain. The sow provides a simple, reproducible, low cost and most frequently used animal model for pelvic floor research. It allows comparison of measurements of mechanical properties with those in the literature. Plus, porcine models are usually used to educate physicians in sphincter injury repair.³²⁻³⁴ Similarly to humans, uterovaginal prolapses are common in sows.^{35,36} In a recent industry study, 21% of sow deaths in the USA could be attributed to pelvic organ prolapse.³⁷

The perineal body is a fibromuscular structure located in the midline of the perineum and provides attachments of the perineal muscles in women.³⁸ Surprisingly, in our experience, sow's perineum seemed to not have a perineal body. In the literature, Bassett et al. is the only article describing the anatomy of sow's perineum.³⁹ They did not report a perineal body. In addition, in the area between the vagina and the rectum of the sow, the only perineal muscle to be described is the anal sphincter. The retractor clitoridis muscle insertion is located in the ventrolateral rectal wall. But, there are no perineal muscles other than the anal sphincter in this area. During our multiple dissections, the full area between the rectum and the vagina was excised, and the skin and the subcutaneous tissue were removed, as described by Kochová et al.⁴⁰ They called the resulting tissue the perineal body. But when we performed the same dissection as described by this research group, it seemed that they took the muscularis of the vagina, the adventitia of the vagina, and fascia-like tissue. Kochová et al. wrote in their work that they did not know the gross anatomy of the structures in the tissue samples. This discrepancy highlights the limits of the sow model. The perineal body can be studied in humans using non-invasive technologies. Zemčík et al. studied the deformation of the perineum during normal delivery using stereophotogrammetry.¹⁰

Chen et al. and Rostaminia et al. studied perineal body stiffness in pregnant and non-pregnant women.^{41,42}

In addition to a relatively small study group, the sow's parity was not known. These sows were nullipara. According to Rynkevici et al. and Drewes et al., biomechanical properties of the vaginal tissue after pregnancy would not recover to those of virgins.^{29,43} These reasons could explain the interindividual variation among the sows. Furthermore, we did not study interactions between each perineal layer. We investigated sow's cadaveric tissues, so postmortem changes must be considered. Indeed, stiffening of muscles appears 2 to 6 h after death because of adenosine triphosphate levels, which cause the binding of the muscle filaments of actin and myosin.⁴⁴ Even if the studied tissues cannot be considered to have intact chemomechanical properties, the results revealed significant differences in biomechanical behavior, providing new insights to better understand the mechanical responses of perineal structures to mechanical stress. In vivo experimentation is not ethical, but in vivo measurements using nondestructive tests should be performed to confirm these results.

5 | CONCLUSION

In these perineal tissue samples of fresh dead sow, the vagina and the anal mucosa were the stiffest tissues. The IAS and EAS were the most extensible and the least stiff. A significantly positive correlation was found between the C1 hyperelastic coefficient and the duration between the first microfailure and the complete rupture of the vagina and between the C1 hyperelastic coefficient and the duration between the first microfailure and the complete rupture of the vagina. No correlation was found for the other perineal tissues. These results must be confirmed on humans using in vivo non-destructive tests.

AUTHOR CONTRIBUTIONS

Marine Lallemand: conceptualization, data curation, formal analysis, methodology, writing—original draft; Tiguida Kadiakhe: conceptualization, data curation, formal analysis, methodology, writing—review; Jérôme Chambert: conceptualization, methodology, writing—review; Arnaud Lejeune: conceptualization, methodology, writing—review; Rajeev Ramanah: writing—review; Nicolas Mottet: writing—review; Emmanuelle Jacquet: conceptualization, methodology, writing—review.

CONFLICT OF INTEREST STATEMENT

The authors have stated explicitly that there are no conflicts of interest in connection with this article.

ETHICS STATEMENT

Sow's perineum were dissected from fresh dead sow provided by local slaughterhouse waste. Animals were not slaughtered for the study. No ethics application was needed because the animals were bred and killed for food production (French decree on the protection of animals used for scientific purposes).

ORCID

Marine Lallemand  <https://orcid.org/0000-0002-3341-5267>

REFERENCES

1. Viannay P, de la Codre F, Brochard C, et al. Prise en charge et conséquences des lésions obstétricales du sphincter anal (LOSA): mise au point. *J Chir Viscérale*. 2021;158:251-262.
2. Attanasio LB, Ranchoff BL, Long JB, Kjerulf KH. Recovery from obstetric anal sphincter injury in a prospective cohort of first births. *Am J Perinatol*. 2022 Jun 30: doi:10.1055/a-1788-4642
3. Thubert T, Cardaillac C, Fritel X, Winer N, Dochez V. Definition, epidemiology and risk factors of obstetric anal sphincter injuries: CNGOF perineal prevention and protection in obstetrics guidelines. *Gynecol Obstet Fertil Senol*. 2018;46:913-921.
4. Pu F, Xu L, Li D, et al. Effect of different labor forces on fetal skull molding. *Med Eng Phys*. 2011;33:620-625.
5. Lapeer RJ, Prager RW. Fetal head moulding: finite element analysis of a fetal skull subjected to uterine pressures during the first stage of labour. *J Biomech*. 2001;34:1125-1133.
6. Bamberg C, Deprest J, Sindhwani N, et al. Evaluating fetal head dimension changes during labor using open magnetic resonance imaging. *J Perinat Med*. 2017;45:305-308.
7. Ami O, Maran JC, Gabor P, et al. Three-dimensional magnetic resonance imaging of fetal head molding and brain shape changes during the second stage of labor. *PLoS One*. 2019;14:e0215721.
8. Silva MET, Oliveira DA, Roza TH, et al. Study on the influence of the fetus head molding on the biomechanical behavior of the pelvic floor muscles, during vaginal delivery. *J Biomech*. 2015;48:1600-1605.
9. Yan X, Kruger JA, Nielsen PMF, Nash MP. Effects of fetal head shape variation on the second stage of labour. *J Biomech*. 2015;48:1593-1599.
10. Zemčík R, Karbanova J, Kalis V, Lobovský L, Jansová M, Rusavy Z. Stereophotogrammetry of the perineum during vaginal delivery. *Int J Gynaecol Obstet*. 2012;119:76-80.
11. Debeer S, Le Luduec J-B, Kaiserlian D, et al. Comparative histology and immunohistochemistry of porcine versus human skin. *Eur J Dermatol*. 2013;23:456-466.
12. Ranamukhaarachchi SA, Lehnert S, Ranamukhaarachchi SL, et al. A micromechanical comparison of human and porcine skin before and after preservation by freezing for medical device development. *Sci Rep*. 2016;6:32074.
13. Khaniki HB, Ghayesh MH, Chin R, Amabili M. Hyperelastic structures: a review on the mechanics and biomechanics. *Int J Non Linear Mech*. 2023;148:104275.
14. Martins PA, Natal Jorge RM, Ferreira AJ. A comparative study of several material models for prediction of Hyperelastic properties: application to silicone-rubber and soft tissues. *Strain*. 2006;42:135-147.
15. Gill PE, Murray W. Algorithms for the solution of the nonlinear least-squares problem. *SIAM J Numer Anal*. 1978;15:977-992.
16. Gabriel B, Rubod C, Brieu M, et al. Vagina, abdominal skin, and aponeurosis: do they have similar biomechanical properties? *Int Urogynecol J*. 2011;22:23-27.
17. Rubod C, Brieu M, Cosson M, et al. Biomechanical properties of human pelvic organs. *Urology*. 2012;79(968):e17-e22.
18. Gajdosik RL. Passive extensibility of skeletal muscle: review of the literature with clinical implications. *Clin Biomech Bristol Avon*. 2001;16:87-101.
19. Wagner HP, Humphrey JD. Differential passive and active biaxial mechanical behaviors of muscular and elastic arteries: basilar versus common carotid. *J Biomech Eng*. 2011;133:051009.
20. Greven K, Rudolph KH, Hohorst B. Creep after loading in the relaxed and contracted smooth muscle (taenia coli of the Guinea pig) under various osmotic conditions. *Pflugers Arch*. 1976;362:255-260.

21. Greven K, Hohorst B. Creep after loading in relaxed and contracted (KC1 or K2SO4 depolarized) smooth muscle (taenia coli of the Guinea pig). *Pflugers Arch*. 1975;359:111-125.
22. Clark-Patterson GL, Buchanan LM, Ogola BO, et al. Smooth muscle contribution to vaginal viscoelastic response. *J Mech Behav Biomed Mater*. 2023;140:105702.
23. Roper JC, Thakar R, Sultan AH. Isolated rectal buttonhole tears in obstetrics: case series and review of the literature. *Int Urogynecology J*. 2021;32:1761-1769.
24. Kay AT, Spirito MA, Rodgerson DH, Brown SE. Surgical technique to repair grade IV rectal tears in post-parturient mares. *Vet Surg*. 2008;37:345-349.
25. Watkins J, Taylor T, Schumacher J. Rectal tears in the horse: an analysis of 35 cases. *Equine Vet J*. 1989;21:186-188.
26. Speirs VC, Christie BA, van Veenendaal JC. The management of rectal tears in horses. *Aust Vet J*. 1980;56:313-317.
27. Dwivedi KK, Lakhani P, Kumar S, Kumar N. A hyperelastic model to capture the mechanical behaviour and histological aspects of the soft tissues. *J Mech Behav Biomed Mater*. 2022;126:105013.
28. Rosenberg K, Trevathan W. Birth, obstetrics and human evolution. *BJOG*. 2002;109:1199-1206.
29. Rynkevic R, Martins P, Hympanova L, Almeida H, Fernandes AA, Deprest J. Biomechanical and morphological properties of the multiparous ovine vagina and effect of subsequent pregnancy. *J Biomech*. 2017;57:94-102.
30. Rynkevic R, Martins P, Andre A, et al. The effect of consecutive pregnancies on the ovine pelvic soft tissues: link between biomechanical and histological components. *Ann Anat Anat Anz*. 2019;222:166-172.
31. Sheard L. Comparing two surgical techniques for repairing third-degree perineal lacerations in postpartum broodmares. *Vet Rec*. 2021;189:e907.
32. Temtanakitpaisan T, Bunyacejchevin S, Koyama M. Obstetrics anal sphincter injury and repair technique: a review. *J Obstet Gynaecol Res*. 2015;41:329-333.
33. Andrews V, Thakar R, Sultan AH. Structured hands-on training in repair of obstetric anal sphincter injuries (OASIS): an audit of clinical practice. *Int Urogynecol J Pelvic Floor Dysfunct*. 2009;20:193-199.
34. Emmanuelli V, Lucot J-P, Closset E, Cosson M, Deruelle P. Development and assessment of a workshop on repair of third and fourth degree obstetric tears. *J Gynecol Obstet Biol Reprod (Paris)*. 2013;42:184-190.
35. Supakorn C, Stock JD, Hostetler C, Stalder KJ. Prolapse incidence in swine breeding herds is a cause for concern. *Open J Vet Med*. 2017;7:85-97.
36. Kiefer ZE, Koester LR, Studer JM, et al. Vaginal microbiota differences associated with pelvic organ prolapse risk during late gestation in commercial sows†. *Biol Reprod*. 2021;105:1545-1561.
37. Ross JW. Identification of putative factors contributing to pelvic organ prolapse in sows (Grant# 17-224). 2019.
38. Siccardi MA, Bordoni B. *Anatomy, Abdomen and Pelvis, Perineal Body*. StatPearls Publishing; 2023.
39. Bassett EG. The comparative anatomy of the pelvic and perineal regions of the cow, goat and sow. *N Z Vet J*. 1971;19:277-290.
40. Kochová P, Hympanová L, Rynkevic R, et al. The histological microstructure and in vitro mechanical properties of pregnant and post-menopausal ewe perineal body. *Menopause*. 2019;26:1289-1301.
41. Rostaminia G, Awad C, Chang C, Sikdar S, Wei Q, Shobeiri SA. Shear wave elastography to assess perineal body stiffness during labor. *Female Pelvic Med Reconstr Surg*. 2019;25:443-447.
42. Chen L, Low LK, DeLancey JO, Ashton-Miller JA. In vivo estimation of perineal body properties using ultrasound quasistatic elastography in nulliparous women. *J Biomech*. 2015;48:1575-1579.
43. Drewes PG, Yanagisawa H, Starcher B, et al. Pelvic organ prolapse in Fibulin-5 knockout mice: pregnancy-induced changes in elastic fiber homeostasis in mouse vagina. *Am J Pathol*. 2007;170:578-589.
44. Martins PALS, Ferreira F, Natal Jorge R, Parente M, Santos A. Necromechanics: death-induced changes in the mechanical properties of human tissues. *Proc Inst Mech Eng*. 2015;229:343-349.

SUPPORTING INFORMATION

Additional supporting information can be found online in the Supporting Information section at the end of this article.

How to cite this article: Lallemand M, Kadiakhe T, Chambert J, et al. In vitro biomechanical properties of porcine perineal tissues to better understand human perineal tears during delivery. *Acta Obstet Gynecol Scand*. 2024;103:1386-1395. doi:[10.1111/aogs.14791](https://doi.org/10.1111/aogs.14791)